

Experimental Test of the Dynamical Coulomb Blockade Theory for Short Coherent Conductors

C. Altimiras, U. Gennser, A. Cavanna, D. Mailly, and F. Pierre*

Phymano team, Laboratoire de Photonique et de Nanostructures (LPN) - CNRS, route de Nozay, 91460 Marcoussis, France

(Dated: September 4, 2021)

We observed the recently predicted quantum suppression of dynamical Coulomb blockade on short coherent conductors by measuring the conductance of a quantum point contact embedded in a tunable on-chip circuit. Taking advantage of the circuit modularity we measured most parameters used by the theory. This allowed us to perform a reliable and quantitative experimental test of the theory. Dynamical Coulomb blockade corrections, probed up to the second conductance plateau of the quantum point contact, are found to be accurately normalized by the same Fano factor as quantum shot noise, in excellent agreement with the theoretical predictions.

PACS numbers: 73.23.-b, 73.23.Hk, 72.70.+m

A tunnel junction exhibits a drop of its conductance at low voltages and temperatures when it is embedded in a resistive circuit, in violation of the classical impedances composition laws. This quantum phenomenon, known as dynamical Coulomb blockade (DCB), results from the excitation of the circuit's electromagnetic modes by the current pulses associated with tunnel events. The theory is well understood and verified experimentally for tunnel junctions [1, 2, 3, 4, 5], but it is only recently that it has been extended to short coherent conductors [6]. The strong recent prediction is that DCB corrections are simply reduced by the *same* normalization factor as quantum shot noise, as a consequence of electron flow regulation by the Pauli exclusion principle [7]. The aim of this work is to perform an accurate experimental test of the DCB theory for coherent conductors and thereby to provide solid grounds to our knowledge of impedances composition laws in mesoscopic circuits.

A powerful description of coherent conductors in absence of interactions is provided by the scattering approach, which encapsulates the complexity of transport mechanisms into the set $\{\tau_n\}$ of transmission probabilities across the conduction channels indexed by n . In short conductors, the energy dependence of $\{\tau_n\}$ can be neglected provided that $h/\tau_{dwell} \gg k_B T, eV_{SD}$, where τ_{dwell} is the dwell time in the conductor, T the temperature and V_{SD} the applied voltage [8]. The conductance then reads $G = G_Q \sum_n \tau_n$, with $G_Q = 2e^2/h$ the conductance quantum; and the current shot noise at zero temperature is $S_I = 2eIF$, where $2eI$ is the Poissonian noise and $F = \sum_n \tau_n(1 - \tau_n)/\sum_n \tau_n$ is the Fano factor. More generally, the full counting statistics of charge transfers can be formulated with $\{\tau_n\}$ [9]. How is this picture modified by Coulomb interaction? First, the low energy excitations are transformed from electrons to Fermion quasiparticles of finite lifetime which thereby limits the coherent extent of conductors [10]. Second, Coulomb interaction couples a coherent conductor to the circuit in which it is embedded, which results in the DCB. In practice, DCB corrections reduce

the transmission probabilities at low energies. The theory of DCB has first been worked out for small tunnel junctions of resistance large compared to the resistance quantum $R_K = h/e^2 \simeq 25.8 \text{ k}\Omega$ and embedded in macroscopic linear circuits characterized by a frequency dependent impedance $Z_{env}(\nu)$ [1, 3]. The theory has been found in excellent agreement with experiments [2], and more recently extended to low impedance [4] and long [5] tunnel junctions. From a theoretical standpoint, tunnel junctions are easy to deal with since they can be treated perturbatively. The generalized DCB theory to short coherent conductors, whose transmission probabilities can take any value between 0 and 1, assumes instead that quantum fluctuations are small. This hypothesis limits its validity to low environmental impedance $\text{Re}[Z_{env}(\nu)] \ll R_K$. The striking prediction is that the amplitude of DCB corrections to the conductance of coherent conductors is reduced relative to tunnel junctions by the same Fano factor as quantum shot noise [6]. Further theoretical investigations concluded that a similar relation holds more generally between the Coulomb corrections to the n th cumulant of current fluctuations and the $(n+1)$ -th cumulant [11]. Experimentally, a pioneer work performed on an atomic contact showed that DCB corrections are strongly reduced when the transmission probability approaches 1, in qualitative agreement with the theory [12]. However, as pointed out by the authors of [12]: “it (was) not possible to conclude whether or not (the theory) is quantitatively correct”. Indeed, at large transmissions, relatively large universal conductance fluctuations were superimposed on the DCB signal whereas, in the tunnel regime, the set of transmission probabilities could not be extracted reliably due to significant DCB corrections. Up to now a quantitative test of the dynamical Coulomb blockade theory for a coherent conductor was missing. The present experiment fills this gap.

In this experiment, we have measured the variations in the resistance of a quantum point contact (QPC) realized in a 2D electron gas (2DEG) while changing the adjustable on-chip circuit in which it is embedded. The con-

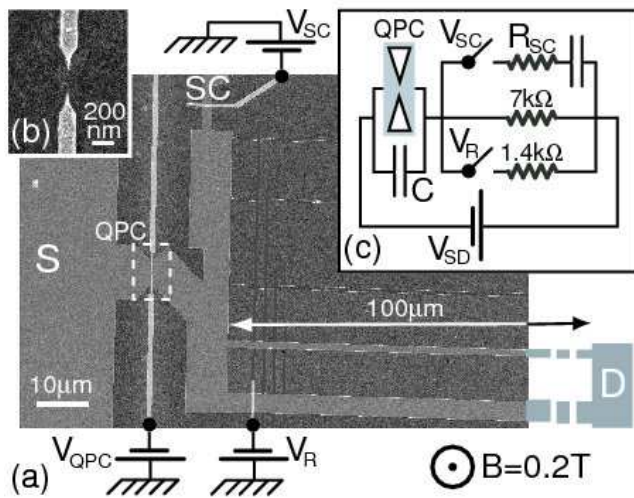


FIG. 1: (a) E-beam micrograph of the sample tailored in a GaAs/Ga(Al)As heterojunction. The 2DEG is patterned by chemical etching, etched areas are darker. Active top metal gates are colorized in the lighter grey. Electrode labels S, D and SC stand respectively for Source, Drain and Short Circuit. (b) Magnified view of the metallic split gate used to tune the QPC. (c) Schematic representation of the sample.

duction channels of a QPC are directly related to the 1D sub-bands quantized by the transverse confinement [13]. By reducing the confinement with voltage biased top gates, the transmission probabilities of the conduction channels are increased continuously and, for adequate geometries [14], one channel at a time. Consequently, the QPC's conductance $G_{QPC} = (n + \tau_{n+1})G_Q$ corresponds to n channels fully transmitted and one channel of transmission probability τ_{n+1} . The knowledge of the transmission probabilities combined with the ability to change them continuously make of a QPC a powerful test-bed for short coherent conductors [15]. As described later, we can change in-situ the circuit surrounding the QPC using voltage biased metallic top gates to deplete the 2DEG underneath. It is by monitoring the QPC's resistance as a function of the circuit impedance that we can extract accurately the amplitude of DCB corrections.

The measured sample, shown in Fig. 1, was realized in a GaAs/Ga(Al)As heterojunction. The 2DEG is 94 nm deep, of density $2.5 \cdot 10^{15} \text{ m}^{-2}$, Fermi energy 100 K and mobility $55 \text{ m}^2 \text{ V}^{-1} \text{ s}^{-1}$. The sample was patterned using e-beam lithography followed by chemical etching of the heterojunction and by deposition of metallic gates at the surface. The QPC is formed in the 2DEG by applying a negative voltage V_{QPC} to the metallic split gates shown in Fig. 1(b). Two stripes of width $1.4 \mu\text{m}$ and $3.8 \mu\text{m}$ [16], and of length $100 \mu\text{m}$, much longer than the electron phase coherence length $L_\phi \sim 10 \mu\text{m}$, were patterned in the 2DEG by chemical etching to form an on-chip resistance in series with the QPC. Measurements were performed in a dilution refrigerator of base temperature

$T = 40 \text{ mK}$. All measurement lines were filtered by commercial π -filters at the top of the cryostat. At low temperature, the lines were carefully filtered and thermalized by arranging them as 1 m long resistive twisted pairs ($300 \Omega/\text{m}$) inserted inside $260 \mu\text{m}$ inner diameter CuNi tubes tightly wrapped around a copper plate screwed to the mixing chamber. The sample was further protected from spurious high energy photons by two shields, both at base temperature. Conductance measurements were performed using standard lock-in techniques at excitation frequencies below 100 Hz. The sample was current biased by a voltage source in series with a 10 M Ω or 100 M Ω polarization resistance at room temperature. Voltages across the sample were measured using low noise room temperature amplifiers. The source (S)-drain (D) voltage was kept smaller than $k_B T/e$ to avoid heating. We applied a small perpendicular magnetic field $B = 0.2 \text{ T}$ [17] to minimize non-ideal behaviors of the QPC such as sharp energy dependence of the transmissions resulting from Fabry-Pérot resonances with nearby defects, and imperfect transmissions across “open” channels.

In our experiment the QPC is embedded in an electromagnetic environment schematically represented as a R//C circuit in Fig. 1(c). The parallel capacitance (C) is the geometrical capacitance between the source electrode (S) and the vertical near rectangular conductor on the right side of the QPC. If the short circuit electrode (SC) is disconnected ($V_{SC} < -0.3 \text{ V}$), the on-chip series resistance can take two values $R_S = 1.2 \text{ k}\Omega$ and $7 \text{ k}\Omega$ depending on whether the wider 2DEG stripe is, respectively, connected ($V_R = 0$) or disconnected ($V_R = -0.35 \text{ V}$), using the metal gate voltage V_R as a switch. If the SC electrode is connected ($V_{SC} \simeq 0$), it acts as a low impedance (R_{SC}) high frequency path to ground in parallel with R_S . Note that DCB reduces the DC conductance of a coherent conductor but that these DCB corrections depend on the impedance of the electromagnetic environment at high frequencies, typically $\nu \sim k_B T/h \in [0.8, 4] \text{ GHz}$ for $T \in [40, 200] \text{ mK}$. Consequently, while the SC electrode is connected at room temperature to a high input impedance voltage amplifier, at high frequencies the environment impedance is expected to be reduced to the on-chip resistance of the SC electrode plus, approximately, the vacuum impedance 377Ω due to antenna effects on length scales larger than a fourth of the electromagnetic wavelength. This is symbolized in Fig. 1(c) by a high frequency impedance R_{SC} in series with a capacitor that acts as a high frequency short circuit.

The experiment was performed as follows: *i*) We first selected a series resistance $R_S = 1.2 \text{ k}\Omega$ or $7 \text{ k}\Omega$ with V_R . *ii*) With the short circuit electrode (SC) connected ($V_{SC} \simeq 0$), we tuned the QPC with V_{QPC} . In this configuration the DCB corrections are minimum because the series resistance R_S is shorted at high frequency by R_{SC} . Since the SC electrode is disconnected from ground at the near DC frequencies applied to measure the sample,

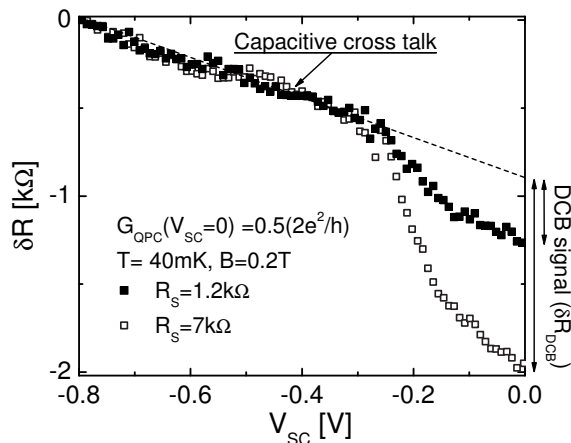


FIG. 2: Resistance variation δR of the QPC in series with the on-chip resistance $R_S = 1.2 \text{ k}\Omega$ (■) or $R_S = 7 \text{ k}\Omega$ (□) plotted versus the voltage V_{SC} that controls the high frequency short circuit (SC) switch (see Fig. 1(c)). For $V_{SC} < -0.3 \text{ V}$ the SC switch is open and δR exhibits a linear dependence with V_{SC} due to the direct capacitive cross talk with the QPC. The DCB signal δR_{DCB} is the difference between the resistance measured at $V_{SC} \simeq 0$ (SC switch closed) and the resistance measured for an open SC switch taking into account the linear capacitive contribution (dashed line).

it could be used to measure separately the QPC and the series resistances. *iii*) We then disconnected the SC electrode by applying a negative voltage V_{SC} , therefore increasing the high frequency circuit impedance and consequently the DCB corrections. By simultaneously measuring the variations of the source (S)-drain (D) resistance, which is the sum of the QPC and the series resistance, we can extract the amplitude of DCB corrections.

Figure 2 shows δR , the resistance variation of the QPC plus the series resistance from their values at $V_{SC} = -0.8 \text{ V}$, plotted versus V_{SC} at $G_{QPC}(V_{SC} = 0) = 0.5G_Q$, $T = 40 \text{ mK}$ and $B = 0.2 \text{ T}$ for $R_S = 1.2 \text{ k}\Omega$ and $7 \text{ k}\Omega$. The dependence of δR with V_{SC} results from two contributions: *i*) At $V_{SC} < -0.3 \text{ V}$ the SC electrode is disconnected and δR is a linear function of V_{SC} with a negative slope that does not depend on R_S . This is a consequence of the capacitive cross talk between the metal gate controlled by V_{SC} and the QPC. We have checked (data not shown) that this slope, which is a non monotonous function of V_{QPC} , is proportional to the derivative of the QPC's resistance with V_{QPC} . The normalization factor $\simeq 10^{-3}$ is in rough quantitative agreement with the sample geometry. *ii*) For $V_{SC} > -0.3 \text{ V}$ we observe, on top of the linear capacitive cross talk, a sudden drop when V_{SC} increases. We attribute this resistance drop, written hereafter δR_{DCB} , to the reduction of DCB corrections as the parallel high frequency short circuit electrode SC gets connected. As expected, δR_{DCB} is larger in the more resistive environment $R_S = 7 \text{ k}\Omega$. In the following we extract δR_{DCB} by measuring the QPC in series with R_S

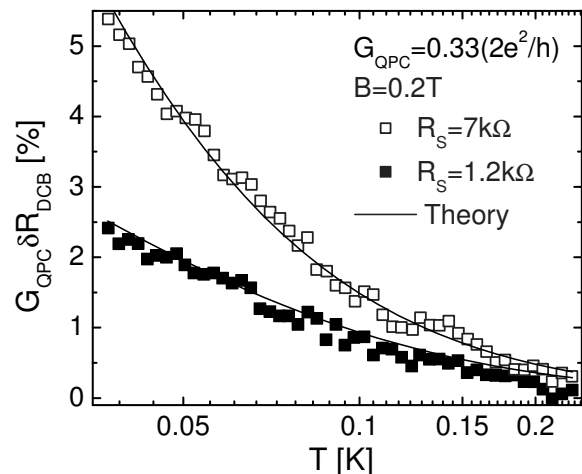


FIG. 3: Measured temperature dependence of relative DCB corrections $G_{QPC}\delta R_{DCB}$ at $G_{QPC} = 0.33G_Q$ and $B = 0.2 \text{ T}$, for $R_S = 1.2 \text{ k}\Omega$ (■) and $R_S = 7 \text{ k}\Omega$ (□). Predictions of the DCB theory are shown as continuous lines. The only fit parameter in the calculation is the high frequency residual resistance of the short circuit path $R_{SC} = 1 \text{ k}\Omega$ (see text).

successively at $V_{SC} = -0.1 \text{ V}$ (SC electrode connected) and $V_{SC} = -0.33 \text{ V}$ (SC electrode disconnected). We then subtract the capacitive cross talk contribution obtained from $\delta R(V_{SC} = -0.56 \text{ V}) - \delta R(V_{SC} = -0.33 \text{ V})$.

Figure 3 shows as symbols the measured temperature dependence of the DCB signal at $G_{QPC}(V_{SC} = -0.1 \text{ V}) = 0.33G_Q$ for $R_S = 1.2 \text{ k}\Omega$ and $7 \text{ k}\Omega$. The continuous lines are predictions of the DCB theory for tunnel junctions [3], normalized by the one-channel Fano factor $F = 1 - G_{QPC}/G_Q \simeq 0.67$. The schematic R//C circuit modeling the QPC's electromagnetic environment is shown in Fig. 1(c). The real part of its impedance plugged into the theory reads $\text{Re}[Z_{env}(\nu)] = R/(1 + (2\pi RC\nu)^2)$. The calculated δR_{DCB} is the difference in the amplitude of DCB corrections for open and closed short circuit switch. The corresponding circuit resistance R is, respectively, $R = R_S$ and $R = 1/(1/R_S + 1/R_{SC})$. The only fit parameter in our calculation is the SC high frequency impedance that we fixed at $R_{SC} = 1 \text{ k}\Omega$, in agreement with the sum of the on-chip SC resistance estimated from the geometry to $600 \pm 100 \Omega$ and the vacuum impedance 377Ω . Other parameters plugged into the DCB calculation are the measured series resistances $R_S = 1.2 \text{ k}\Omega$ or $R_S = 7 \text{ k}\Omega$ and the geometrical capacitance $C = 30 \text{ fF}$ estimated numerically with an accuracy of $\pm 5 \text{ fF}$ [18]. The very good agreement between data and theoretical predictions provides a strong support to our interpretation and allows us to now compare the measured dependence of DCB on transmission probabilities with the predicted Fano reduction factor.

To test the generalized dynamical Coulomb blockade theory, we measured the relative amplitude of DCB corrections versus the QPC conductance at 40 mK and for

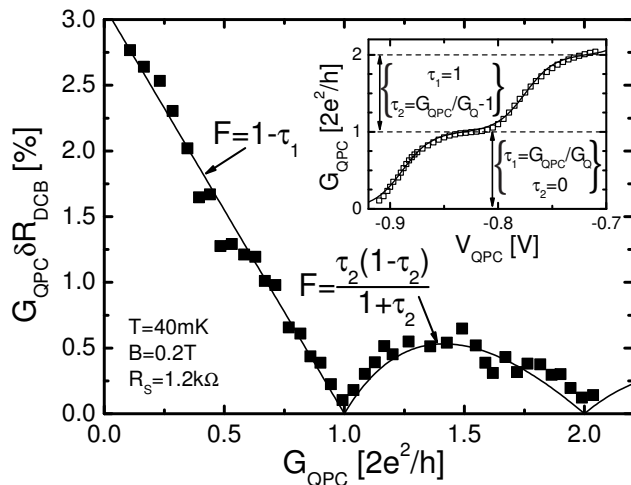


FIG. 4: Measured relative DCB corrections (■) plotted versus the QPC conductance. The continuous line is the predicted reduction by the Fano factor $F = \frac{\sum_n \tau_n (1 - \tau_n)}{\sum_n \tau_n}$. Inset: Measured QPC conductance (□) plotted versus the split gate bias voltage V_{QPC} . The best fit using a quadratic confinement potential [14] is shown as a continuous line.

$R_S = 1.2 \text{ k}\Omega$ [19] (see Fig. 4). The predictions depend on the set $\{\tau_n\}$, it is therefore crucial to extract accurately the transmissions probabilities of the QPC. The inset in Fig. 4 shows the QPC conductance up to $2G_Q$ versus the split gate voltage V_{QPC} , measured at $T=40 \text{ mK}$ and $B=0.2 \text{ T}$. We subtracted 350Ω from the data to account for the residual DC series resistance by adjusting the first three plateaus on multiples of the conductance quantum [20]. From the maximum deviation between our data and the best fit (continuous line in inset of Fig. 4) using Büttiker's model of QPCs [14], we estimate our accuracy on the transmission probabilities $\{\tau_1 = \min[1, G_{QPC}/G_Q], \tau_2 = \max[0, G_{QPC}/G_Q - 1]\}$ to be better than 0.05. The continuous line in Fig. 4 shows the relative amplitude of DCB as predicted by theory [6]. We observe an excellent quantitative agreement between the data and the Fano factor $F = (\tau_1(1 - \tau_1) + \tau_2(1 - \tau_2)) / (\tau_1 + \tau_2)$ that controls quantum shot noise [15].

To conclude, we have performed a quantitative experimental test of the generalization of dynamical Coulomb blockade theory to short coherent conductors embedded in low impedance circuits. We find dynamical Coulomb blockade corrections that are reduced in amplitude by the same Fano factor as quantum shot noise, in quantitative agreement with the predictions. This result is not only important within the fundamental field of quantum electrodynamics in mesoscopic circuits. It also provides solid grounds to engineer complex devices with coherent conductors and to use dynamical Coulomb blockade as a tool to probe the transport mechanisms. For this purpose DCB has the advantage on shot noise that the signal

increases when the probed energies decrease.

The authors gratefully acknowledge inspiring discussions and suggestions by D. Estève, P. Joyez, H. Pothier and C. Urbina. We also thank M.H. Devoret, F. Portier and B. Reulet for stimulating discussions and G. Faini, R. Giraud and Y. Jin for permanent assistance. This work was supported by the ANR (ANR-05-NANO-039-03) and NanoSci-ERA (ANR-06-NSCI-001).

* Corresponding author: frederic.pierre@lpn.cnrs.fr

- [1] M.H. Devoret *et al.*, Phys. Rev. Lett. **64**, 1824 (1990); S.M. Girvin *et al.*, Phys. Rev. Lett. **64**, 3183 (1990).
- [2] A.N. Cleland *et al.*, Phys. Rev. B **45**, 2950 (1992); T. Holst *et al.*, Phys. Rev. Lett. **73**, 3455 (1994).
- [3] For a review see G.-L. Ingold and Y.V. Nazarov, in *Single Charge Tunneling*, edited by H. Grabert and M.H. Devoret (Plenum, New York, 1992), Chap. 2.
- [4] P. Joyez *et al.*, Phys. Rev. Lett. **80**, 1956 (1998).
- [5] F. Pierre *et al.*, Phys. Rev. Lett. **86**, 1590 (2001).
- [6] D.S. Golubev and A.D. Zaikin, Phys. Rev. Lett. **86**, 4887 (2001); A. Levy Yeyati *et al.*, Phys. Rev. Lett. **87**, 046802 (2001).
- [7] Th. Martin and R. Landauer, Phys. Rev. B **45**, 1742 (1992).
- [8] M. Büttiker and R. Landauer, IBM J. Res. Dev. **30**, 451 (1986).
- [9] See Y.M. Blanter and M. Büttiker, Phys. Rep. **336**, 1 (2000) and references therein.
- [10] D. Pines and P. Nozière, *The Theory of Quantum Liquids* (W.A. Benjamin, New York, 1966); For a recent review on phase coherence of electrons in diffusive metals see F. Pierre *et al.*, Phys. Rev. B **68**, 085413 (2003).
- [11] A.V. Galaktionov *et al.*, Phys. Rev. B **68**, 085317 (2003); M. Kindermann and Y.V. Nazarov, Phys. Rev. Lett. **91**, 136802 (2003); M. Kindermann *et al.*, Phys. Rev. B **69**, 035336 (2004); I. Safi and H. Saleur, Phys. Rev. Lett. **93**, 126602 (2004).
- [12] R. Cron *et al.*, in *Electronic Correlations: From Meso to Nano-Physics*, edited by T. Martin, G. Montambaux, and J. Trân Thanh Vân (EDP Sciences, Les Ulis, 2001), p. 17; R. Cron, PhD Thesis (available on <http://tel.ccsd.cnrs.fr/>), Université Paris 6 (2001).
- [13] L.I. Glazman *et al.*, JETP Lett. **48**, 238 (1988).
- [14] M. Büttiker, Phys. Rev. B **41**, 7906 (1990).
- [15] M. Reznikov *et al.*, Phys. Rev. Lett. **75**, 3340 (1995); A. Kumar *et al.*, Phys. Rev. Lett. **76**, 2778 (1996).
- [16] The 2DEG width is about 700 nm narrower due to lateral depletion near the edges.
- [17] Shubnikov-de Haas oscillations of $R_S(B)$ are negligible up to the applied magnetic field $B=0.2 \text{ T}$.
- [18] The code was provided gracefully by D. Estève.
- [19] For $R_S = 7 \text{ k}\Omega$ and $G_{QPC} > 0.5G_Q$, non negligible universal conductance fluctuations of $R_S(V_{SC})$ forbade us to extract the DCB signal accurately.
- [20] The corresponding reduction of G_{QPC} is at most 2.5% and 5% below, respectively, the first and second plateau.